Mirage Simulation: An Investigation into Thermal Refraction

Connor Legg, Declan Bracken, Michael Sieroka

Department of Physics, Engineering Physics & Astronomy, Queen's University, Kingston, ON, Canada

Submitted December: 5th, 2021

Abstract

The objective of this experiment is to test and refine a model for the continuous refraction of light through a homogenous medium with a temperature gradient to simulate the effects of a mirage. To quantize the physics of mirages and compare with theoretical modelling, a thermal gradient was applied vertically across a tank of water and used to refract the beam of a laser pointer over a short (~1 meter) distance into a digital camera. Over the course of 62 minutes the beam's peak displacement was found to be 10.0 ±0.5 mm through a peak temperature gradient of 0.35 ± 0.05 °C/m, which significantly overshoots the approximate model by 628%. This result demonstrates the expected trend in behavior of light but concludes that the assumption of thermodynamic linearity in the temperature gradient may be inaccurate for modelling the behavior of the system.

1. Introduction

Snell's law is a well-studied equation that models the refraction of light as it discretely passes from one medium to another. The more complex application of refraction, light passing through a continuous medium, is less intuitively understood despite its frequent occurrence in natural and fabricated systems, such as mirages and collimating waveguides. This experiment tests a model of the refraction of light across a continuous medium to provide insight on this phenomenon. Modelling such a system entails the application of Snell's law to a continuum of mediums (or a gradient of some extrinsic property across a homogenous medium) to describe the continuous refraction of a beam. Once a continuous form of Snell's law is derived (Section 3.1), a function describing the index of refraction along the beams path must be established to allow for its application in practice. In the case of this experiment the function related the temperature of water to its index of refraction using a Cauchy equation (Section 3.2). The temperature of the water was extrapolated from the continuous data of three temperature probes placed at different heights in the tank based on the assumption of a linear thermal gradient.

2. Experimental Apparatus

The primary purpose of the apparatus was to generate a temperature gradient in a fluid through which a laser could be continuously refracted. The temperature gradient was initially designed to be as large as possible, ranging from -196 to over 100 ^{o}C to create maximal deflection, but the safety concerns around such extreme temperatures caused the team to reconsider and instead focus on precise measurement methods to eliminate the need for large gradients. The original experimental design relied on air as a

fluid medium to reflect the conditions of a mirage as closely as possible, but air's low density and thermal conductivity made the size of potential deflections small making measurement difficult. As the design progressed a liquid medium was decided upon to reduce chaotic flow, increase density, and make containment easier. Speculation into accessible transparent liquids with strong correlations between temperature and index of refraction yielded glycerol solutions and vegetable oil as the most viable options. However, after the initial testing of the camera system revealed its ±0.26 mm accuracy allowing significant data to be drawn from water's projected deflection values, these options were rejected in favor of water for simplicity.

2.1 Main System

The gradient was designed to be vertical with the heat source at the top and cold reservoir at the bottom to prevent convection. The water tank in the main system was 80 cm by 40 cm by 10 cm with 6mm thick plexiglass walls, a copper plate floor, and 3 sets of 2cm tall feet spaced evenly along its length. The dimensions of the tank were long and thin to allow for a large path length for the beam to increase refraction while keeping the volume of water in the tank low and reduce heating requirements. The initial tank for the main system had a far larger volume which would have required a longer period to reach temperature equilibrium and needed a higher surface area heating element to evenly heat the top surface of the water. The water tank was placed in a large shallow plastic tub which was filled with an ice water bath up to the level of the tank's copper floor plate, creating a conductive connection to the cold reservoir. Initially liquid nitrogen was chosen as the cold source, but with the selection of water as the refracting medium the temperature became implausible as it could cause freezing. The heating element was a ½ inch copper pipe suspended just below the surface of the water tank connected to the heating system by ½ inch PVC tubing fastened with hose clamps to prevent leaks.

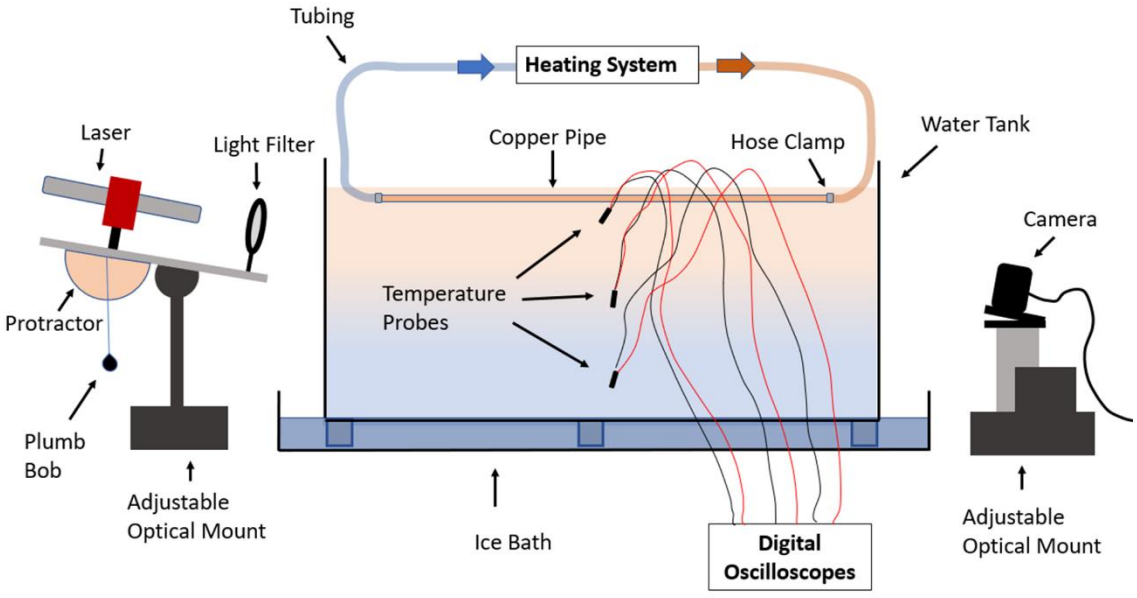

Figure 1: Main system apparatus diagram.

2.2 Heating System

The heating system was a separate isolated water tank with a VWR 1112A heat pump and two 150W aquarium heaters bringing the water temperature up to a stable 52.5 ± 0.1°C and pumping it through the copper pipe in the main system. The temperature of 60 °C was chosen as a maximum threshold for the heating system to reduce the risk of elevated temperature exposure and to ensure the tubing remained well below its operating threshold of 75 °C.

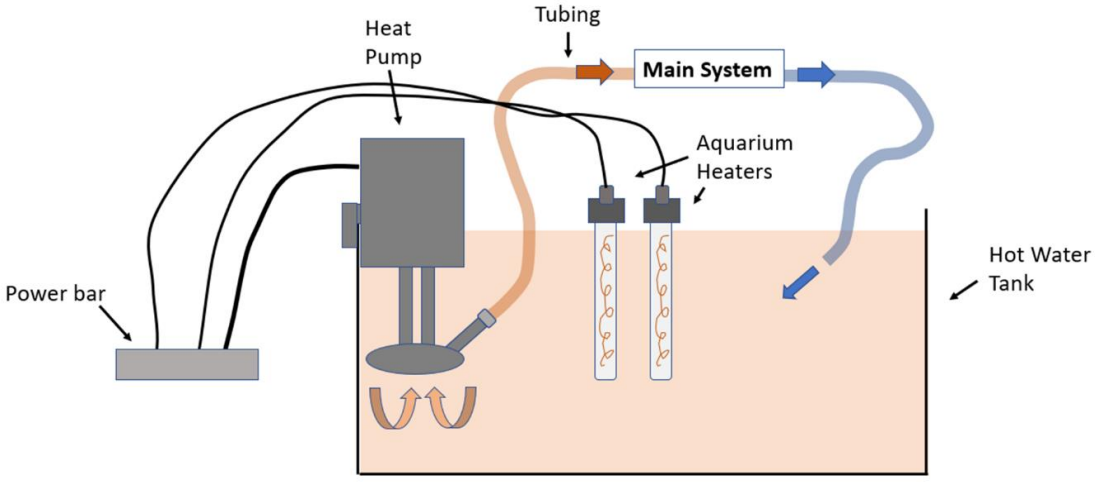

Figure 2: Heating system apparatus diagram.

2.3 Laser System

The laser system was an optical stand with a rod attached to a tiltable mount where a class 2, 650 nm wavelength laser and two neutral density filters (Codes FIL143 and FIL163) were fastened in series. To measure the angle of the initial beam a protractor and a plumb bob were attached to the bottom of the rod. Additional considerations for the laser system were a small zip tie used to toggle the laser into the on position, an easily removable filter to allow for convenient alignment of the beam and the camera, and removal of the zip tie whenever the laser was not mounted to reduce the risk of retinal damage.

2.4 Camera System

The first proposed measurement system was recording results on a piece of paper at the end of the tank by hand, but after the first displacement predictions from the model were calculated to be on the millimeter scale, this was discounted as far too inaccurate to yield valuable data and an optical sensor was adopted. The final imaging system was a model N5 camera sensor (U4-2180) attached to the top of a vertically adjustable optical mount fastened to the table using clamps. The vertical range of the Optical sensor was 3.67 mm, which could encompass the 1.56mm deflection predicted by the model (Section 3.0), but vertical adjustment was still built into the setup to ensure the entirety of the signal was visible to the sensor throughout its deflection and allow measurements should the deflection be greater than predicted. The 30mm vertical range of the optical mount bridged gaps between any large deflections of the beam while the 177 pixels/mm sensor located the specific center of the beam, resulting in an overall camera system accuracy of ± 0.26mm, making this the highest accuracy measurement in the experiment. An additional consideration for the camera system was the taping over of its internal LEDs to prevent their diffused light from interfering with the signal of the laser.

3. Model and Predictions

Modelling of the physical system before conducting experimental research was necessary to justify overall feasibility. Producing such a model provided the freedom to vary experimental parameters in the interest of safety and simplicity while maintaining the ability to produce relevant data.

3.1 Continuous Snell's Law

To estimate an expected order of magnitude for laser deflection, a preliminary model was developed in MATLAB using a derivation of the continuous form of Snell's law [1]. A linear thermodynamic gradient is assumed for feasibility of the model. The final equation used to calculate the position, x, of a refracted beam path through a medium is seen below.

$$x = l * ln(k(1 + sin(\alpha))/(k - y \pm \sqrt{(k-y)^2 - l^2})) \quad (1)$$

$$l = kcos(\alpha) \quad (2)$$

$$k = n_0 a / v_0 \quad (3)$$

Where n_0 is the initial index of refraction at the entry edge of the tank, a is the length of the tank, u_0 is the net change in refractive index across the tank, and α is the initial angle of the beam above the horizontal. x and y are the position coordinates of the laser.

Included in the simulation are parameters varying the entry point of the laser into the tank, the tank dimensions, the refraction through both ends of the plexiglass, the thickness of the plexiglass, and the distance between the camera sensor and the tank, as well as the variation in temperature values.

3.2 Cauchy Formula for Index of Refraction

Temperature values are converted to refractive indices using a Cauchy formula with experimentally determined temperature dependent coefficients and the wavelength of the laser pointer (650 nm) [2]. The full function can be found in the Appendix.

$$n(\lambda, t) = A(t) + B(t)/\lambda^2 + C(t)/\lambda^4 + D(t)/\lambda^6 \quad (4)$$

Where the coefficients A, B, C and D are Cauchy coefficients given by the equations:

$$B = 5208.2413 - 0.5179t - 2.284 * 10^{-2}t^2 + 6.9608 * 10^{-5}t^3 \quad (5)$$

$$A = 1.3208 - 1.2325 * 10^{-5}t - 1.8674 * 10^{-6}t^2 + 5.0233 * 10^{-9}t^3 \quad (6)$$

$$C = -2.5551 * 10^{8} - 18341.336t - 917.2319t^2 + 2.7729t^3 \quad (7)$$

$$D = 9.3495 + 1.7855 * 10^{-3}t + 3.6733 * 10^{-5}t^2 - 1.2932 * 10^{-7}t^3 \quad (8)$$

3.3 Expected Results

The following is a full accounting for the parameters used in the experiment applied to the model. The dimensions of the tank are unchangeable and measured as 785x315x100 ±1 mm (length by height by width). The angle of the beam into the tank is held constant at 19° ± 1° below horizontal and the laser enters the tank 30 ± 1 mm below the water level, the camera sensor is placed 249 ±3 mm from the edge of the tank, and the thickness of the plexiglass is 6 ±1 mm. The Index of refraction in air and plexiglass are taken as 1.0003 and 1.495, respectively, and the non-heated tank temperature is taken as 23°C, the recorded ambient room temperature throughout the experiment [3],[4]. A catalog of expected results is

presented in the Table below for sample temperature gradients and a sample graph from the model is shown in Figure 3.

Table 1: Modeled beam displacements for a variety of sample temperature gradients.

Temp Range (°C)	Refractive Index Range (10^-4)	Beam Spot Displacement (mm)
10° - 20°	6.78	0.97
10° - 30°	17.00	2.34
10° - 40°	30.00	4.09

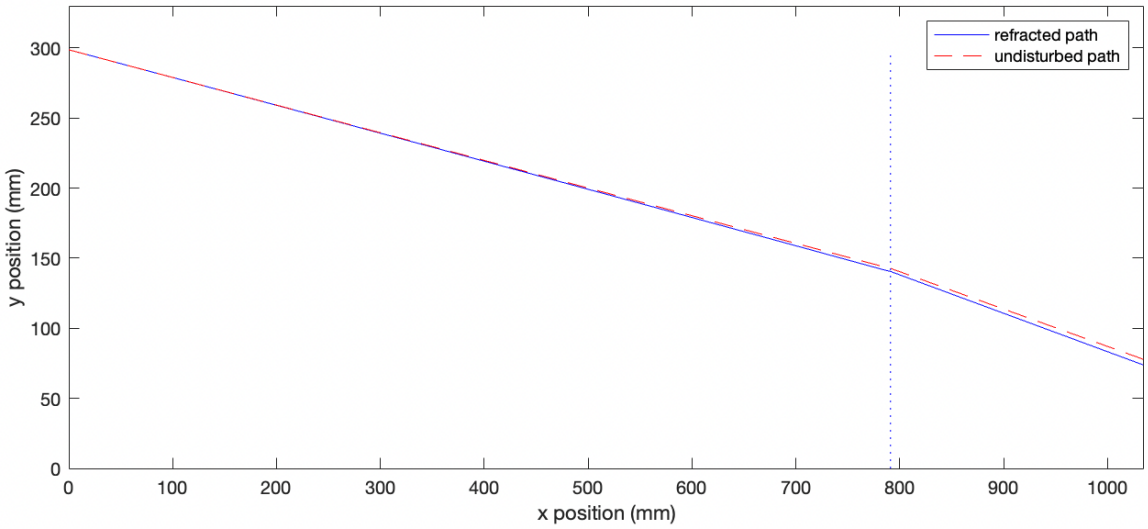

Figure 3: sample graph from the continuous Snell's Law model.

4. Experimental Procedure

4.1 Initial Setup

To begin the experiment, secure the three temperature probes in the main system tank at a low, middle, and high point, recording their heights (Table 2). Next, fill the hot water and main system tanks with water to 15 cm and 5 cm below the top rim, respectively. Ensure the copper pipe is suspended above and aligned with the top of the main system (not submerged yet), turn on both aquarium heaters, and turn the heat pump on to low speed and 50 °C. From now until the end of the lab be careful not to touch the copper pipe as it will be hot. Next, connect the three thermal probes to three different multimeters, labelling the probes for post-lab calibration. Set the multimeters to read for voltage and turn on the diode mode so that the current remains constant. Connect the camera sensor to a computer and align the laser so that the signal populates the lower portion of the sensor reading without truncating on the bottom of the screen. Place neutral density filters in series with the laser until the sensor reading does not saturate when there is no other light in the room. For reference in later calculations, record all relevant lengths, initial positions, and the angle of the laser (Listed in Table 3). Just before starting the experiment wipe the inside and outside edges of the tank where the laser will pass through to remove air bubbles and dirt that might interfere with the laser's signal. Once the heating system has stabilized (~52 °C) you may proceed with the experiment.

4.2 Beam Deflection Process

Place the zip tie over the laser button to hold it in the on position and begin recording the camera sensor output and all three multimeter readings simultaneously so that the data is synchronized for post-lab analysis. Fill the basin underneath the narrow tank with ice until just below the copper base of the main system tank and top off the basin with freezing water until just above the copper base. Now carefully lower the copper pipe into the top of the main system tank so that is just barely submerged. Once this setup is complete turn all lights off. The laser will now begin visibly displacing on the camera sensor as a gradient is formed between the ice bath and the hot copper rod. Once the laser reaches the top of the camera sensor range, adjust the optical mount vertically to realign the laser at the bottom of the sensor, recording the optical mount height measurements before and after and the time of the adjustment. Note, this adjustment should be done with the lights on to prevent mistakes and should be completed quickly to reduce the amount of data that is corrupted by the additional light source. If at any point the cold reservoir runs low on ice, add more ice to ensure it remains at a constant temperature; the hot reservoir has enough input power to remain at constant temperature throughout the experiment and does not need to be as closely monitored. Repeat this adjustment procedure until the camera reading is stable, indicating the system has reached thermal equilibrium.

4.3 Final Actions

Once the experiment is complete, stop the recordings, remove the zip tie from the laser, and turn off all the heating system components. After adequate time has passed for the heating system to cool down, the system may be deconstructed. Next, the three temperature probes must be calibrated using a two-point calibration with samples of liquid nitrogen and boiling water. One at a time, place each probe in the liquid nitrogen and boiling water and record the stable voltage reading on the multimeter (again on the diode setting). Be sure not to touch the edges of the containers with the probes as it will affect the voltage reading. Using the stable voltage values and the temperatures of the liquids, a linear relationship between voltage and temperature can be established and used to solve for the temperature readings of the probes from the lab data.

5. Experimental Results

Over the course of 01:02:49 ± 5 seconds, the maximum displacement of the beam spot on the camera sensor was found to be 10 ± 0.4 mm. The beam spot's position over time for 5-minute intervals is recorded in Table 4 in the appendix and visualized in Figure 4 below. The relative beam displacement is calculated according to equation 9, where the coefficient 1.75/330 is the pixel to millimeter conversion factor and 666 is the total size, in pixels, of the camera sensor. Relative displacement, stage position, and pixel position are kept to 3 significant figures to avoid data destruction despite their uncertainty.

$$\Delta y = pos_{stage} + (666 - pos_{pix}) * \frac{1.75}{310} - y_0 \tag{9}$$

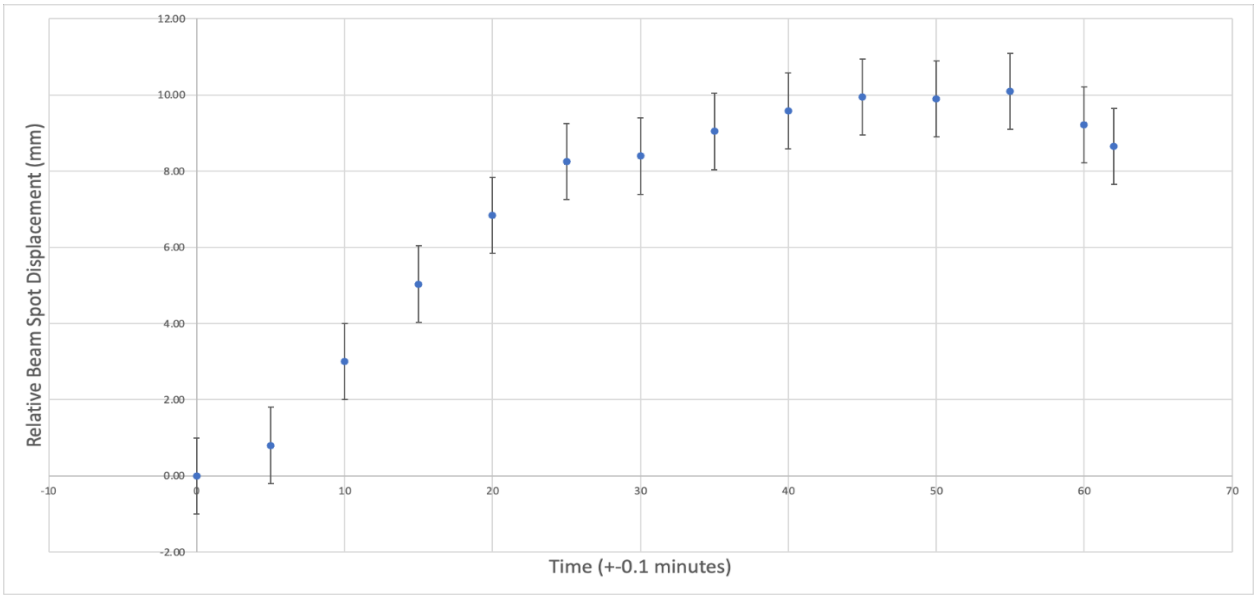

Figure 4: Experimental laser beam deflection over time.

Figure 5 shows images of the beam spot on the camera sensor moving downward vertically over the course of 3:13 minutes near the beginning of the experiment. Note the image from the camera is inverted, making the spot appear to move upwards.

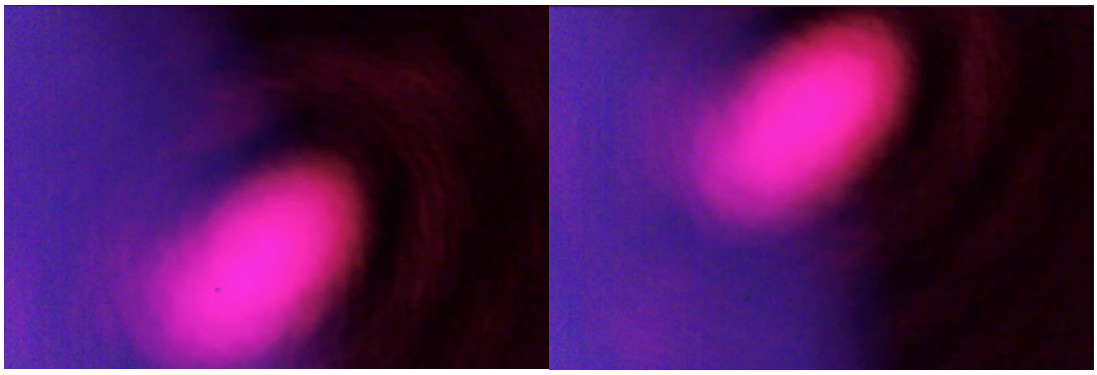

Figure 5: Beam Deflection over First Adjustment Period5

At 00:52:30 the heating pump was turned off and the beam spot began to reverse direction for the final 8 minutes and 30 seconds of the experiment. Figure 6 below shows the beam position with time stamps during this process.

Figure 6: Beam Refraction Maxima and Subsequent Regression

Calibrated temperature data recorded from the probes is plotted over the same 5-minute time interval in Figure 7. The net gradient between the top to middle, and the bottom to middle probes are plotted in Figure 8 in degrees per cm and used in parallel with the probe positions in Table 2 to linearly extrapolate the net temperature gradient of the tank. The extrapolated temperatures of the top and bottom of the tank are plotted in Figure 7 alongside the original probe data.

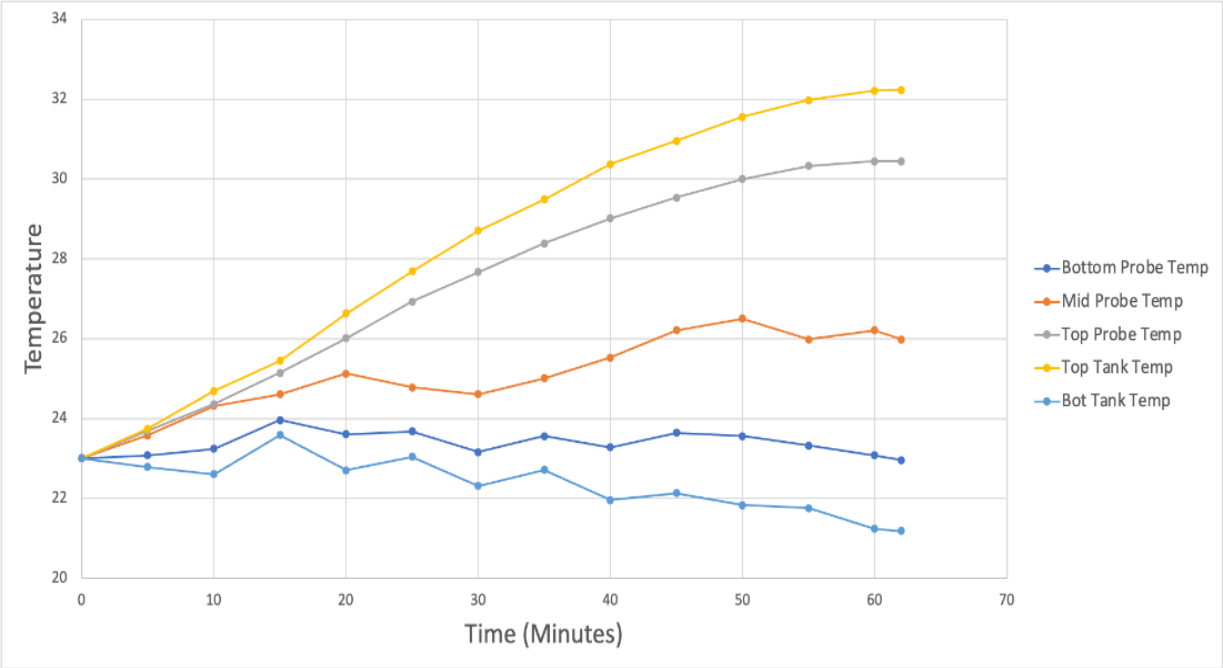

6

Figure 7: Temperature probe readings in the water tank over time.

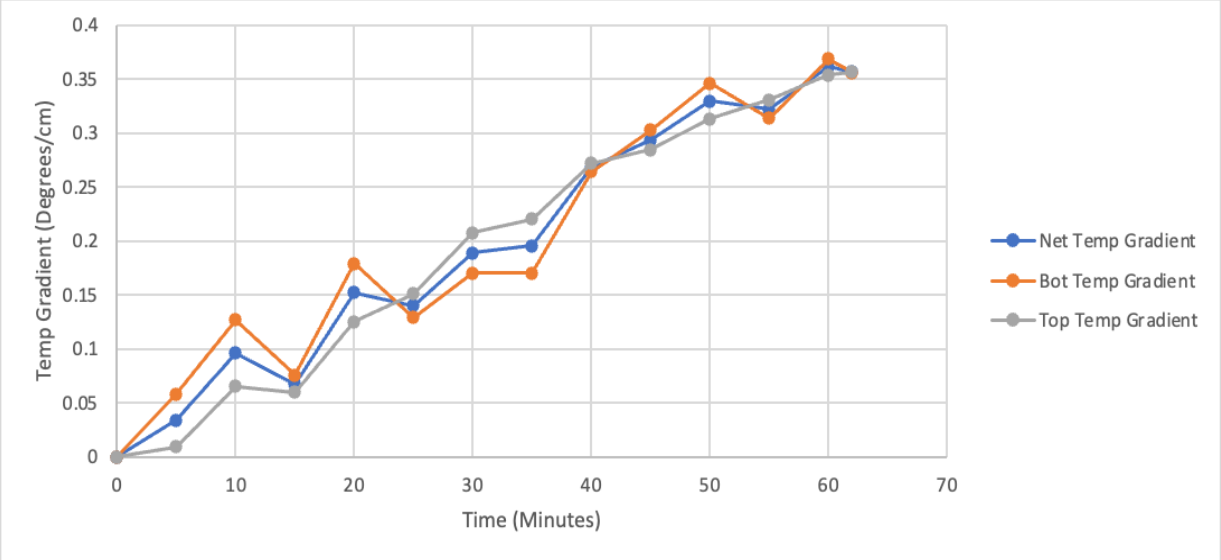

Figure 87: Temperature gradients in the water tank over time.

The extrapolated temperature data is used for theoretical modelling of the beam displacement over time, the experimental and theoretical results are compared in Figure 9 as a function of the net temperature gradient.

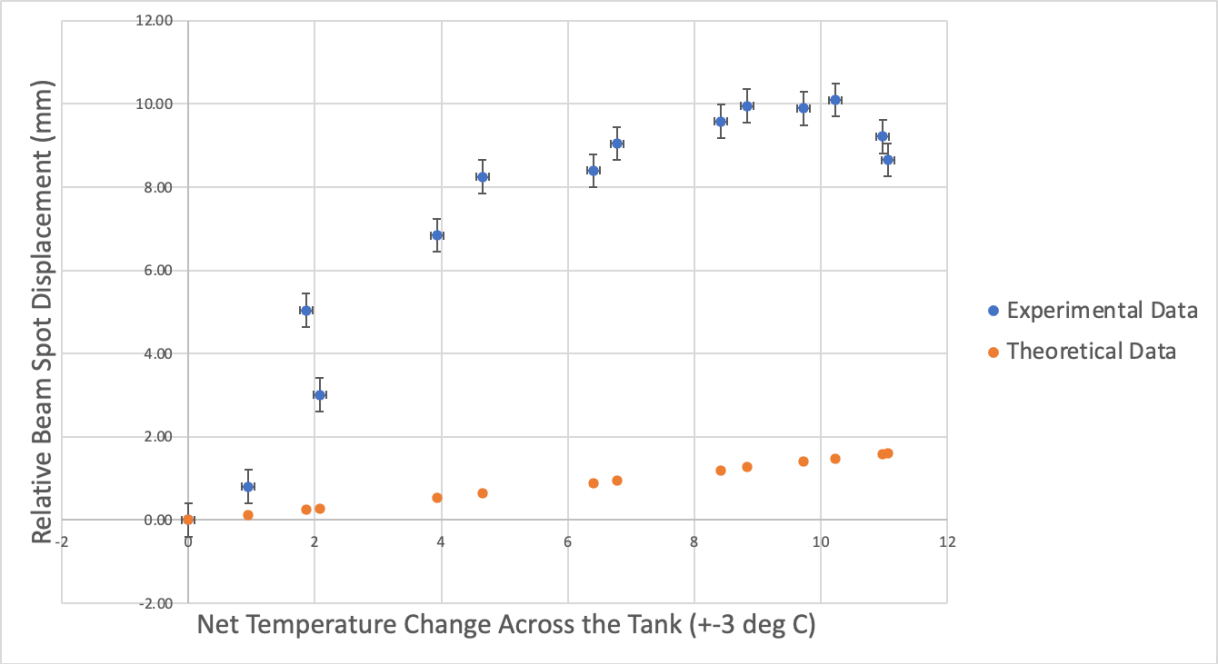

Figure 98: Experimental and modeled beam deflection as a function of the temperature gradient.

6. Analysis

The experimental results qualitatively demonstrate the expected behavior of continuous light refraction through a thermal gradient. After submerging the heating element in the tank and filling the cold reservoir the beam began to move, requiring numerous vertical adjustments of the camera's optical mount to contain the beam in the range of the camera sensor (Figure 5). As the tank approached thermal equilibrium, the rate of beam displacement depreciated notably until reaching a plateau attributable to final equilibrium, as seen in Figures 9. This behavior matches that data recorded by the thermal probes which all began at room temperature and diverged to their equilibrium values at decreasing rates until plateauing (Figure 7). At minute 52:30 the heat pump was turned off, stopping the flow of heated water through the copper pipe. Approximately 2:30 minutes later equilibrium was achieved, and the peak beam displacement was measured at 10.0 ± 0.4 mm, with a net temperature variation across the tank of 11 ± 3 °C. This displacement drastically overshoots the expected value of 1.59 mm using the same temperature gradient in the numeric model with 628% error. The system continued to behave as expected for the remainder of the experiment when the beam spot reversed directions because of cooling (Figures 6, 9).

The discrepancy between the beam spot's behavior as a function of temperature gradient questions model validity. Uncertainty in system parameters such as tank length and height, sensor position, beam angle, laser wavelength, and temperature which are core variables in modelling cannot be varied within a reasonable range to account for the near order of magnitude shift in theoretical and experimental

results. The displacement output by the model given the maximized uncertainties present in the physical system is 2.17 mm, which leaves 460% error compared to experimental results. The application of a continuous Snell's law derivation through a medium of variable refractive index is the most probable cause for error. Other modelling components such as the path of light through the plexiglass and air have a minimal effect on output while also being mathematically simplistic. The most obvious issue is assuming a linear thermal gradient. It is one of the few physical errors unaccounted for and is necessary for the applied derivation to be true.

Assume the thermal gradient resembles a 3rd degree polynomial rather than a linear function, where close proximity to either heat exchanger produces a very steep gradient and through the center of the tank the gradient flattens. If this is the case, then the temperature at the top of the tank and bottom would increase by a much larger factor since the linear extrapolation method used would undermine the actual exponential relationship. We can use the linear model to approximate this theory by implementing the same peak temperatures, but over a much smaller tank height. What we find is that by reducing the tank height to 80 mm rather than 330, the displacement of the beam spot increases to an expected value of 8.93 mm. This result requires major assumptions about the nature of the system but could be a significantly contributing factor to the discrepancies found between the model and the experiment.

7. Discussion and Future Work

A significant limitation of the model used in this lab is the assumption of a linear temperature gradient. The model required a linear temperature gradient to compute results, but this is unlikely to occur in a legitimate application and proves difficult to replicate in the lab. To achieve the linear gradient for this experiment, the temperatures of the ice bath and copper pipe would have to have been held constant until an equilibrium was reached for each data point. This process would have taken too long and was not feasible given the three-hour window available for individual experiments. Consequently, approximations were made by assuming the temperature gradient in the water tank was linear. Other limitations include the many sources of error in the apparatus' setup such as, the initial laser angle, the equipment dimensions, and the accuracy of the temperature readings. However, despite the large uncertainties in some of these measurements, some form of measurement error is unavoidable and their contribution to the uncertainty in the final data was far less than the contribution of the linear temperature gradient approximation. Overall, these limitations resulted in the experimental data not following the theoretical model.

Moving forward, the model used for this experiment could be adapted or extended to be used for different applications. The current model is a continuous version of Snell's Law with added parameters specific to our apparatus. However, Snell's Law is broad and is applicable for several kinds of waves and mediums. As a result, the model could be changed to calculate wave path and deflection for many situations if given the correct starting parameters such as, initial wave angle, the temperature gradient, path length, etc. Applications include modeling sound waves instead of light or using the medium of air to model mirages which was the initial motivation of this experiment. If a highly accurate measurement of a non-linear temperature gradient could be achieved the Snell's law model could be mathematically adapted to compute the deflection. Alternatively given a deflection and a set of temperature data points an advanced algorithm based off of continuous Snell's law could calculate the form of the gradient.

8. Conclusion

This experiment first modeled the continuous deflection of a laser through the temperature gradient of a homogenous medium and subsequently designed an experiment to observe whether this behavior would hold in non-ideal conditions. Experimental results demonstrated that the laser followed expected behavior but with a significantly different magnitude of deflection than the theoretical model. The laser refracted as the temperature gradient increased and stopped when the gradient stagnated. The final displacement of the beam spot on the sensor was 8.65 ± 0.5 mm, but for the same gradient the model predicted a deflection of just 1.59 mm. The most appropriate explanation for these discrepancies has been narrowed to the assumption of a linear temperature gradient which could not be replicated experimentally. In the future, this model derived from the continuous Snell's Law could be adapted to find the deflection of alternative waves through different mediums so long as the medium is homogenous, and an approximation of a linear thermal gradient can be made.

.

9. Appendix

Table 2: Temperature Probe Height Measurements.

Bottom Probe Height	9.5 ±0.05cm
Middle Probe Height	18 ±0.05cm
Top Probe Height	30.5 ±0.05cm

Table 3: Measurements of the System

Laser Distance:	22.2 ±0.05cm	Tank Length:	78.5 ± 0.5 cm
Laser Angel:	19 ± 1^{o}	Wall Thickness:	0.6 ±0.05cm
Laser height:	38.2 ±0.05cm	Water Level:	35.0 ±0.05cm
Camera Distance:	24.9 ±0.05cm	Height of Laser Incidence:	30.25 ±0.05cm
Camera Height:	14.8 ±0.05cm	Copper Floor Height:	2.5 ±0.05cm

Table 4: Laser beam net deflection over time given the parameters of stage position, pixel position and beam position.

Time (± 0.1 min)	**Stage Position (± 0.2 mm)**	**Pixel Position (± 10 pixels)**	**Beam Position (mm)**	**Relative Displacement (mm)**	**Displacement Uncertainty**
0	0	200	2.63	0.00	0.5
5	1.25	280	3.43	0.80	0.5
10	2.75	155	5.63	3.00	0.5
15	6.25	415	7.67	5.04	0.5
20	8.25	450	9.47	6.84	0.5
25	8.25	200	10.88	8.25	0.5
30	9.75	440	11.03	8.40	0.5
35	9.75	325	11.68	9.04	0.5
40	9.75	230	12.21	9.58	0.5
45	9.75	165	12.58	9.95	0.5
50	11.25	440	12.53	9.90	0.5
55	11.25	405	12.72	10.09	0.5
60	11.25	560	11.85	9.22	0.5
62	11.25	660	11.28	8.65	0.5

```
function disp = LASERFUNK2(v)
%vartiable parameters
L = v(1);
a = v(2);
D_sensor = v(3);
T_water = v(4);
T_bot = v(5);
T_top = v(6);
lambda = v(7);
thicc = v(8);
n_a = v(9);
n_g = v(10);
alpha = v(11);
ystart = v(12);

a1 = a;
N = 20001; %resolution

n = ref_ind(T_water,lambda); %index of refraction for no thermal gradient
nf = ref_ind(T_bot,lambda); %initial index of refraction
n01 = ref_ind(T_top,lambda); %final index of refraction
alpha = alpha*pi/180; %initial angle of laser from horizontal
ystart = 30;

startglass = 1; %if going through plexiglass

%Air - Glass
if startglass == 1
    theta1 = asin(n_a/n_g*sin(alpha)); %calculate refractive angle through glass
    ystart = thicc*tan(theta1)+ystart;

    %Glass - Water
    n0 = nl_2(n01,nf,ystart,a); %return index of refraction at height ystart of the tank
    alpha = asin(n0/n_g*sin(theta1)); %calculate initial angle in liquid
end

%recalculate the starting position and refractive index
n0 = nl_2(n01,nf,ystart,a);
a = a-ystart;

y = zeros(1,N);

%use derivation deffinitions
u0 = n0-nf;
k = n0*a/u0;
l = k*cos(alpha);

%iterate using independant variable y
x = linspace(0,L,N);

%calculate x positions of beam path depending on
y = -(exp(x./l).*(l.^2 - k.^2 + (k - exp(-x./l).*(k + k.*sin(alpha))).^2))./(2.*(k + k.*sin(alpha)));

xlin = zeros(1,4);
xlin(1:2) = linspace(0,L,2); %undisturbed paths
xlin(3:4) = [L+thicc,L+thicc+D_sensor];
ylin(1:2) = xlin(1:2)*tan(alpha)+ystart;

theta2 = atan((y(end) - y(end-1)) / (x(end) - x(end-1))); %approximate output angle
n02 = nl_2(n0,nf,y(end),a); %get output index of refraction
    %Water - Glass
theta3 = asin(n02 / n_g * sin(theta2)); %calculate
x = horzcat(x,L+thicc);
y = horzcat(y,y(end)+thicc * tan(theta3));
    %Glass - Air
theta4 = asin(n_g / n_a*sin(theta3));
x = horzcat(x, x(end) + D_sensor);
y = horzcat(y, y(end) + D_sensor*tan(theta4));

theta5 = asin(n / n_g * sin(alpha)); %output angle through plexiglass
ylin(3) = ylin(2) + thicc * tan(theta5);
xlin(3) = L+thicc;
theta6 = asin(n_g / n_a * sin(theta5));
xlin(4) = xlin(3) + D_sensor;
ylin(4) = ylin(3) + D_sensor * tan(theta6);

y = y+ystart;

disp = abs(ylin(end)-y(end));

plot(x,y,'b',xlin,ylin,'r--')
xlabel("x position (mm)")
ylabel("y position (mm)")
```

Figure 10: MATLAB code for the continuous Snell's Law model.

10. References

[1] Tatum, J. *Differential Form of Snell's Law*, University of Victoria, (2021) Accessed November 24th 2021 <https://phys.libretexts.org/@go/page/8292 >

[2] Bashkatov, A. and Genina, E. *Water refractive index in dependence on temperature and wavelength: A simple approximation*. Proceedings of SPIE - The International Society for Optical Engineering. 5068. (2003) 10.1117/12.518857.

[3] Stone, J. A. and Zimmerman, J. H., *Index of Refraction of Air*, Engineering Metrology Toolbox (2001) Accessed November 23rd, 2021, <http://emtoolbox.nist.gov/Wavelength/Documentation.asp>

[4] Kasarova S. N. et al., *Analysis of the dispersion of optical plastic materials*, Filmetrics (2007) Accessed November 15th, 2021, <https://www.filmetrics.com/refractive-index-database/Acrylic/Acrylate-Lucite-Perspex-Plexiglass >

[5] Greenler, R. G., *Laboratory simulation of inferior and superior mirages,* Journal of Optical Society of America 4, 589-590 (1987) < https://doi.org/10.1364/JOSAA.4.000589>

[6] James, O. C., *Optical Refractive Index of Air: Dependence on Pressure, Temperature and Composition,* Applied Optics 6, 51-59 (1967) Accessed November 2nd 2021, <https://doi.org/10.1364/AO.6.000051 >

[7] Ritland, H. N., *Relation Between Refractive Index and Density of a Glass at Constant Temperature,* Journal of the American Ceramic Society, 38: 86-88 (1955) <https://ceramics.onlinelibrary.wiley.com/doi/10.1111/j.1151-2916.1955.tb14581.x>

[8] Schricker, A. (2001), *Refractive Bending of Light due to Thermal Gradients in Air,* European Laboratory for Particle Physics (CERN), Accessed October 28th 2021, <https://cds.cern.ch/record/684258/files/muon-2001-017.pdf>

[9] M. Vollmer and R. Tammer, *Laboratory experiments in atmospheric optics,* Applied Optics 37, 1557-1568 (1998) < https://doi.org/10.1364/AO.37.001557 >